



# Effect of short range ferromagnetic interaction on magnetocaloric properties of polycrystalline $\text{Eu}_{0.55}\text{Sr}_{0.45}\text{MnO}_3$ compound



Dipak Mazumdar<sup>a,\*</sup>, Kalipada Das<sup>b</sup>, I. Das<sup>a</sup>

<sup>a</sup> CMP Division, Saha Institute of Nuclear Physics, HBNI, 1/AF-Bidhannagar, Kolkata 700 064, India

<sup>b</sup> Department of Physics, Seth Anandram Jaipuria College, 10, Raja Naba Krishna Street, Kolkata 700005, India

## ARTICLE INFO

### Keywords:

Manganites

Magnetocaloric effect

Clausius-Clapeyron equation

## ABSTRACT

Magnetic and magnetocaloric properties of polycrystalline  $\text{Eu}_{0.55}\text{Sr}_{0.45}\text{MnO}_3$  compound have been investigated. In addition to the field induced meta-magnetic transition, magnetically a mixed ground state (ferromagnetic and antiferromagnetic) was observed especially at the low temperature ( $T < 30$  K). Influence of the predominant short range ferromagnetic interaction reflects in its magnetocaloric effect, calculated from Maxwell's thermodynamic relation. However, different nature of the magnetocaloric effect, calculated using Clausius-Clapeyron equation, discussed considering the phase diagram of this material. Our study suggest, in contrast to the Maxwell's relation, magnetocaloric parameter ( $-\Delta S$ ) derived from Clausius-Clapeyron equation gives the reliable value, useful for magnetic refrigeration cycle.

## 1. Introduction

In present days magnetocaloric effect (MCE) have been gained an utmost attention from its technological and fundamental aspects [1–9]. To substitute the environmentally harmful gas compression cooling, searching of suitable magnetic refrigerant materials is become a great issue to the researchers [10–14]. On the other hand from the magnetocaloric effect, the nature of the magnetic ground state can also be probed easily [15–20]. Measure of the suppression of magnetic randomness in magnetic materials in the presence of external magnetic field is quantified as the isothermal magnetic entropy change ( $\Delta S(T)$ ). The nature of the interaction in magnetic ground state can be understood from the variation of the isothermal magnetic entropy change in temperature landscape [16,21,22]. For ferromagnetic (FM) materials, generally  $-\Delta S(T)$  shows positive values with a peak at ordering temperature. However, positive to negative cross-over in  $-\Delta S(T)$  is appeared in case of antiferromagnetic (AFM) materials which is ascribed as inverse magnetocaloric effect (IMCE). The fascinating nature of  $-\Delta S(T)$  is also appeared in case of the magnetically mixed phase materials [8,15,23–25]. Depending upon the temperature and external magnetic field, the fraction of the different competing magnetic phase changes and induced this change in the nature of  $-\Delta S(T)$  [26–30].

From the fundamental as well as the technological perspectives, doped perovskite manganites achieved considerable attention parallel to the intermetallic compounds [2,8,31,32]. Over the intermetallic

compounds, there are also some beneficial aspects for manganite materials namely lower cost, high chemical stability, small eddy current loss etc. [2,32,33]. Moreover, electronic band width induced tunability of the disorder-order transition in doped perovskite manganite is an another important commercial aspects [6,13,31,34]. During previous two decades, the magnetocaloric effect of  $\text{La}_{1-x}\text{Ca}_x\text{MnO}_3$ ,  $\text{La}_{1-x}\text{Sr}_x\text{MnO}_3$  and  $\text{Pr}_{1-x}\text{Ca}_x\text{MnO}_3$  were extensively studied [2,8,35–41]. Metal-insulator transition, charge ordering, predominant ferromagnetism, canted magnetic state etc. are found in above mentioned manganites for appropriate values of bivalent doping concentration 'x' [42–45].

There are several methods to calculate the magnetocaloric entropy change both theoretically and experimentally for long range ordered materials [1,46–50]. However, for phase separated materials having different competing ground states, the calculation procedure of magnetocaloric effect is slightly different [16,28–30]. Especially for the materials having first order magnetic phase transition, the change of magnetic entropies calculated both experimentally and theoretically, are contradicted from each other [54,51–53]. Such differences may be ascribed due to the conversion of the non equilibrium nature of the competing phase fractions. Similar arguments should also valid for the materials having short range magnetic interaction. In this case the ground state magnetization value depends on the measurement protocols.

In the doped perovskite manganite families having short range ferromagnetic interaction, polycrystalline  $\text{Eu}_{0.55}\text{Sr}_{0.45}\text{MnO}_3$  is one of the

\* Corresponding author.

E-mail address: [dipak.mazumdar@saha.ac.in](mailto:dipak.mazumdar@saha.ac.in) (D. Mazumdar).

<https://doi.org/10.1016/j.jmmm.2020.166507>

Received 14 November 2019; Received in revised form 9 January 2020; Accepted 23 January 2020

Available online 25 January 2020

0304-8853/© 2020 Elsevier B.V. All rights reserved.

most well studied compound [54–60]. Earlier studies indicate that a series of magnetic transition take place depending upon the temperature and external magnetic field [56,58]. At low temperature, field induced metamagnetic transition appears for  $H > 2.3$  T magnetic field (antiferromagnetic to ferromagnetic) [58]. Due to the presence of predominant short range interaction, temperature dependent magnetization, measured in different protocols exhibited different behavior especially at low temperature region.

In this paper, we have carried out magnetic and magnetocaloric effect study for the polycrystalline  $\text{Eu}_{0.55}\text{Sr}_{0.45}\text{MnO}_3$  compound. Magnetocaloric entropy change ( $\Delta S(T)$ ) was calculated by using Maxwell's thermodynamic relation and Clausius–Clapeyron equation. Along with significant values of  $-\Delta S(T)$  and Relative Cooling Power (RCP), different behavior of  $-\Delta S(T)$  was found at low temperature in two different calculation procedure. Such distinct nature of  $-\Delta S(T)$  was addressed considering its magnetic phase diagram constructed from the isothermal magnetization data.

## 2. Sample preparation and characterization

The polycrystalline  $\text{Eu}_{0.55}\text{Sr}_{0.45}\text{MnO}_3$  (ESMO) has been prepared by well-known conventional solid-state reaction method by using high purity  $\text{Eu}_2\text{O}_3$  (99.99%),  $\text{SrCO}_3$  (99.995%) and  $\text{MnO}_2$  (99.9%) powders.  $\text{Eu}_2\text{O}_3$  was preheated at 800 °C for 12 h. to remove any moisture or  $\text{CO}_2$  present in it. Stoichiometric mixture of all the compounds was calcined in the temperature range 1000 °C–1200 °C for 60 h. with intermediate grinding for homogenization. At the end, the resultant product was reground, pelletized using hydrostatic pressure and sintered at 1350 °C for another 48 h, then furnace cooled down to room temperature.

For structural characterization, X-ray diffraction (XRD) study was performed on the powder form of the sample by using  $\text{Cu-K}\alpha$  radiation in Rigaku-TTRAX-III diffractometer. Magnetic Properties of the sample were measured in a vibrating sample mounting based Superconducting Quantum Interference Device (SQUID-VSM) from Quantum Design.

## 3. Results and discussions

To check the phase purity and crystal structure of the as prepared sample, X-ray diffraction (XRD) experiment of the powdered sample has been carried out at room temperature using a  $\text{Cu-K}\alpha$  source (having wavelength 1.54 Å) on a TTRAX-III powder diffractometer from M/s Rigaku. The structural analysis (profile fitting) of the as recorded XRD spectrum have been performed on the basis of Rietveld analysis using FULLPROF software. The profile fitted data and the experimental X-ray spectrum along with the Bragg positions are shown in Fig. 1(a). As revealed by the Rietveld analysis, the sample has a single phase in nature with orthorhombic unit cell having Pbnm space group. Within the whole diffraction range, we did not notice any impurity peak. The extracted lattice parameters are  $a = 5.470$  Å,  $b = 5.424$  Å, and  $c = 7.667$  Å, which are very close to the earlier reported values [58,59].

We have also carried out the X-ray diffraction at low temperatures to check the temperature induced structural transition of this compound. X-ray diffraction patterns at some selected temperatures are shown in Fig. 1(b). The temperature dependent X-ray diffraction patterns indicate that there is no signature about the temperature induced structural transition down to  $T = 15$  K. However, the peak positions were shifted with temperature due to the change of the crystallographic unit cell parameters.

To explore the information about the magnetic ground state, we have recorded the magnetization in different measurement protocols which are described as follows.

•**ZFCW**: sample was first cooled down (from 300 K to 5 K) in the absence of any external magnetic field and magnetization data were recorded during warming cycle in the presence of desired static magnetic field.

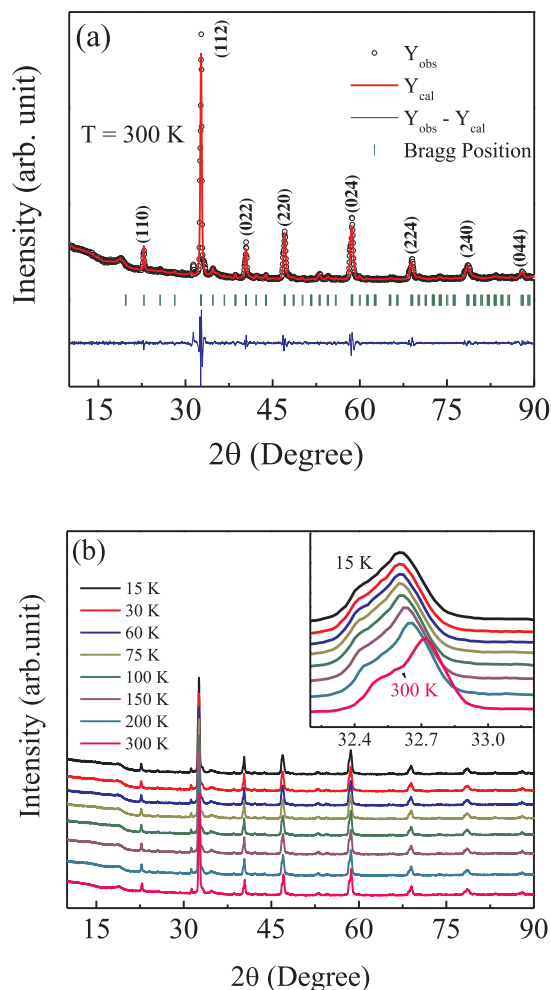
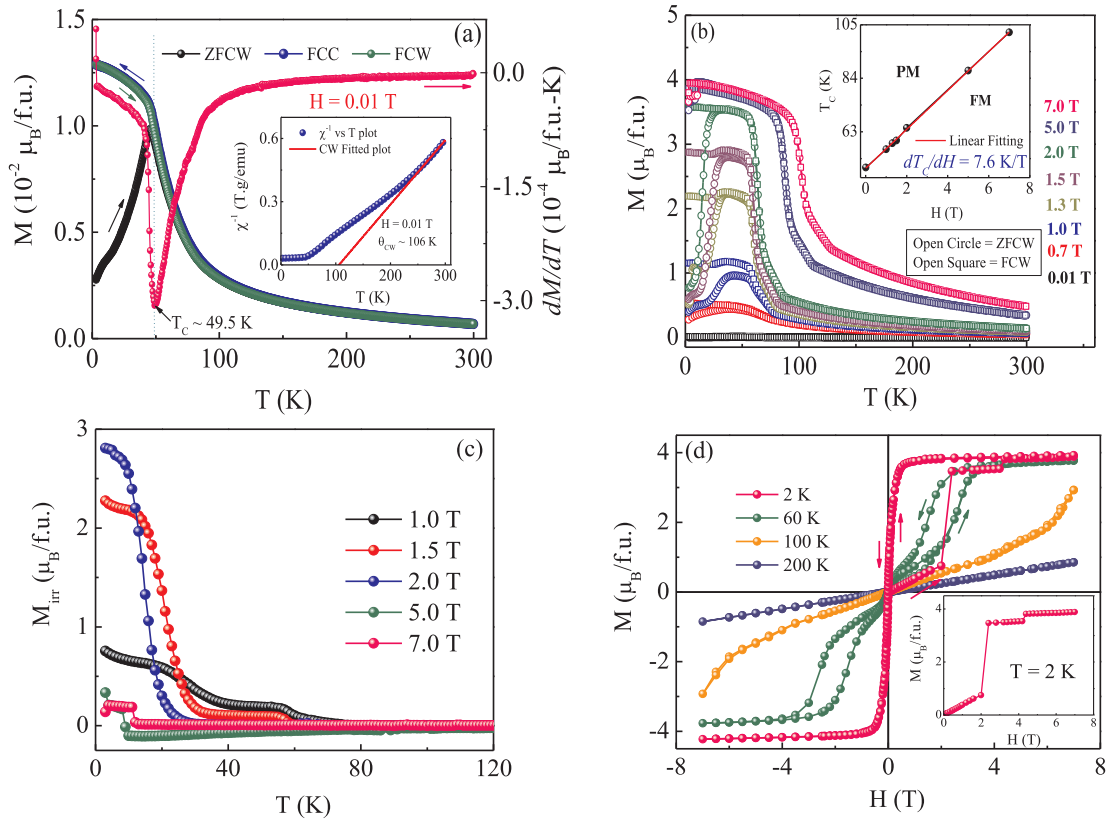


Fig. 1. (a) Reitveld profile refinement of the XRD spectrum of powdered polycrystalline ESMO compound recorded at 300 K, (b) Temperature dependent powdered X-ray diffraction spectrum of ESMO compound. Inset shows the magnified view of more intense peak of the compound.

•**FCC**: in this protocol, magnetic field was applied at room temperature and magnetization was recorded during cooling cycle (from 300 K to 5 K).

•**FCW**: sample was cooled down in the presence of external magnetic field and magnetization data were recorded during warming cycle in the presence of same (as applied during cooling) external magnetic field.

Magnetization as a function of temperature in three different protocols in presence of very low magnetic field ( $H = 0.01$  T) is shown in Fig. 2(a). Temperature dependent derivative of magnetization indicates the ferromagnetic like transition near  $T_C = 50$  K (shown in Fig. 2(a)). In addition to that the bifurcation between ZFCW and FC curves is predominant below 50 K temperature. In case of such a sample having short range ferromagnetic correlation, the irreversible nature of magnetization is expected [61,62]. To understand the effect of external magnetic field, we have carried out magnetization as a function of temperature at different external magnetic fields in both ZFCW and FCW protocols. Our experimental outcome indicates that the bifurcation is predominant below  $T = 5$  T external magnetic field. However for  $H = 5$  T and 7 T, the bifurcation between ZFCW and FCW is reduced as shown in Fig. 2(b). Field induced paramagnetic to ferromagnetic transition temperature ( $T_C$ ) also increases with the increase of magnetic field values at the rate of 7.6 K/T which is plotted in the inset of Fig. 2(b). The inverse susceptibility ( $\chi^{-1}$ ) as a function of temperature shows non-linear behavior as shown in the inset of Fig. 2(a). By using



**Fig. 2.** (a) Temperature dependence of magnetization measured at 0.01 T external applied magnetic field in three different protocols ZFCW, FCC and FCW. Arrows represent the corresponding directions. Pink color curve in the same figure represent the  $dM/dT$  versus  $T$  plot. Inset shows the variation of inverse susceptibility ( $\chi^{-1}$ ) as a function of temperature along with the Curie–Weiss law fitted curve, (b) Variation of magnetization with respect to temperature in presence of different external magnetic fields. Inset shows the  $T_c - H$  phase diagram, (c) Temperature dependence of irreversible magnetization ( $M_{irr} = M_{FC} - M_{ZFC}$ ) for various magnetic fields, (d) Magnetic field dependence of magnetization measured at  $T = 2$  K, 60 K, 100 K and 200 K during the field change  $0 \rightarrow 7$  T  $\rightarrow -7$  T  $\rightarrow 7$  T. Inset indicates the enlarged view of M-H isotherm at  $T = 2$  K.

the Curie–Weiss (C-W) law of the form  $\chi = C/(T-\theta_{CW})$  in the paramagnetic region, where  $C = \mu_{eff}^2/3k$  is the Curie constant and  $\theta_{CW}$  stands for paramagnetic Curie–Weiss temperature, the curve is fitted linearly. The theoretical effective magnetic moment ( $(\mu_{eff})_{theo}$ ) of the compound has been calculated using the following formula,

$$(\mu_{eff})_{theo} = \sqrt{0.55 * (\mu_{eff})_{Mn^{3+}}^2 + 0.45 * (\mu_{eff})_{Mn^{4+}}^2}$$

where,  $(\mu_{eff})_{Mn^{3+}}$  and  $(\mu_{eff})_{Mn^{4+}}$  are calculated with the formula,  $\mu_{eff} = g\sqrt{j(j+1)}\mu_B$ . The observed effective magnetic moment ( $(\mu_{eff})_{obs}$ ) has been calculated from the linear fitting of  $\chi^{-1}$  vs  $T$  plot in the paramagnetic region (i. e. from Curie constant,  $C = (\mu_{eff})_{obs}^2/3k$ ). The value of  $(\mu_{eff})_{theo}$  is  $4.465 \mu_B/f.u.$  and the value of  $(\mu_{eff})_{obs}$  is  $7.41 \mu_B/f.u.$ . Since,  $(\mu_{eff})_{obs} > (\mu_{eff})_{theo}$  and the positive values of  $\theta_{CW} = 106$  K confirms the presence of short-range ferromagnetic interaction in the paramagnetic region of the sample.

The temperature dependence of irreversible magnetization ( $M_{irr} = M_{FCW} - M_{ZFCW}$ ) [16,30] at different external magnetic fields is shown in Fig. 2(c). The variation of irreversible magnetization ( $M_{irr}$ ) is conspicuous below  $T = 60$  K which is suppressed at very high temperature. In addition to that the maximum value of  $M_{irr}$  appears at intermediate field range. Such nature indicates that in the presence of the strong external magnetic field, FM ground state stabilized and hence  $M_{irr}$  is suppressed.

To get a clear view of the nature of magnetic ground state, study of the variation of magnetization as a function of magnetic field must be required. As a result, we have measured magnetic field dependence of magnetization at  $T = 2$  K, 60 K, 100 K and 200 K as shown in Fig. 2(d). At  $T = 2$  K, magnetization increases linearly with increasing magnetic

field represents the presence of a canted AFM like ground state of the compound. The system undergoes a metamagnetic transition at  $H \sim 2$  T which initiated the growth of FM domains present in the sample [58]. With further increasing of magnetic field, another sharp jump observed at  $H \sim 4.2$  T (shown in the inset of Fig. 2(d)). This may be due to the presence of magnetically mixed phases in the sample where alone 2 T magnetic field is not sufficient to align the AFM moments along the applied field direction which required 4.2 T magnetic field to completely align the magnetic moments. This whole scenario may be understood considering the martensitic like transition [47,63,64]. There is a field hysteresis present in the sample at  $T = 60$  K. This kind of hysteresis represents the coexistence of multiple magnetic phases in a system [65–67]. With further increasing temperature, thermal energy initiated to loose the blockage of magnetic spins and as a result the system converted into a paramagnetic (PM) one which reflects in the field dependence of magnetization measured at  $T = 200$  K. From the above results, we can conclude that the ground state of the system consists of multiple magnetic phases like canted AFM or AFM and FM, but with application of magnetic field the undisturbed charge-order AFM states are started melting and in a particular magnetic field, it will be completely converted into a FM one. And the whole process is irreversible in nature.

Generally, magnetic field induced metamagnetic transition is temperature sensitive. To estimate the required critical fields at different temperatures, we have measured magnetic field dependent magnetization at different temperatures. Regarding this point one thing is necessary to mention that before each isothermal magnetization measurement, the system was warmed up to 200 K (well above its FM transition temperature) to remove the effect of any previous

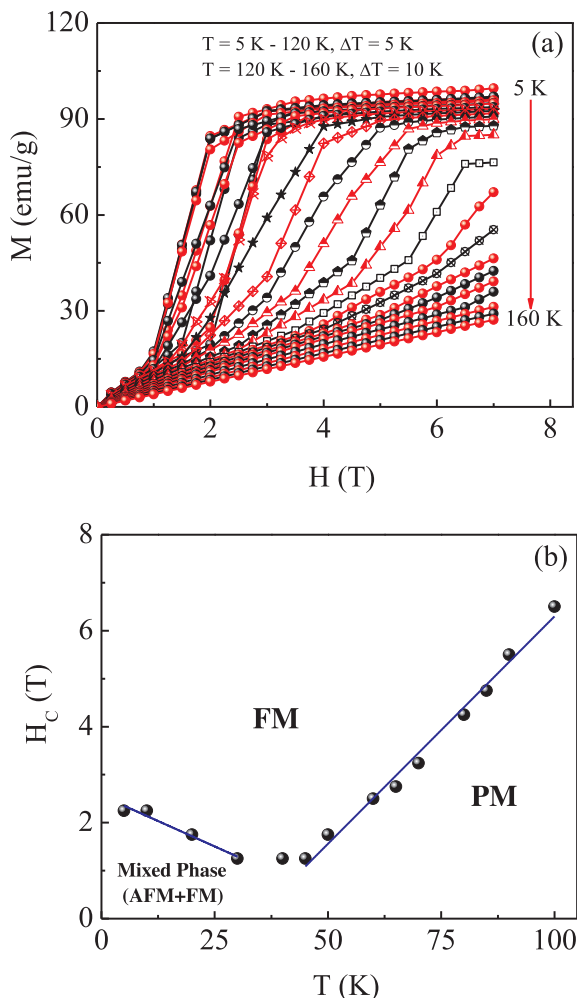


**Fig. 3.** (a) Isothermal magnetization curves measured at various temperatures over the field range 0–7 T, (b)  $H_c - T$  phase diagram calculated from the isotherms as shown in Fig. 3(a).

measurements if any present. The magnetic isotherms at different temperature is given in Fig. 3(a). We have extracted the critical field for metamagnetic transition by taking derivative (with respect to field) of magnetization curves. The critical magnetic field at different temperature is plotted in Fig. 3(b). The solid lines in Fig. 3(b) is only for guide to the eye. At very low temperature region ( $T < 25$  K), the critical magnetic field required to take place the metamagnetic phase transition increases with decreasing temperature. Such nature indicates the dominant multi-magnetic interaction at low temperature region. Additionally, Wang et al. reported the spin-glass nature of the same compound at low temperature region ( $T < 50$  K) [58]. However at slightly high temperature region, the required critical magnetic field increases with increasing temperature almost linearly. This nature suppress the ferromagnetic nature of the compound. To summarize the magnetic properties of the ESMO compound, it exhibits a field induced metamagnetic transition from mixed phase (FM + AFM) to FM or PM to FM depending upon the temperature. At low temperature region especially below 25 K, the required field for metamagnetic transition is 2.5 T as shown in Fig. 3(b). To visualize the nature of evolution of magnetic state in different external fields more systematically, we have calculated the magnetic entropy change at different external magnetic field.

From the isothermal magnetization data, the magnetic entropy change ( $\Delta S$ ) can be calculated by using classical Maxwell's thermodynamic relation (MXR) [46] which is given below

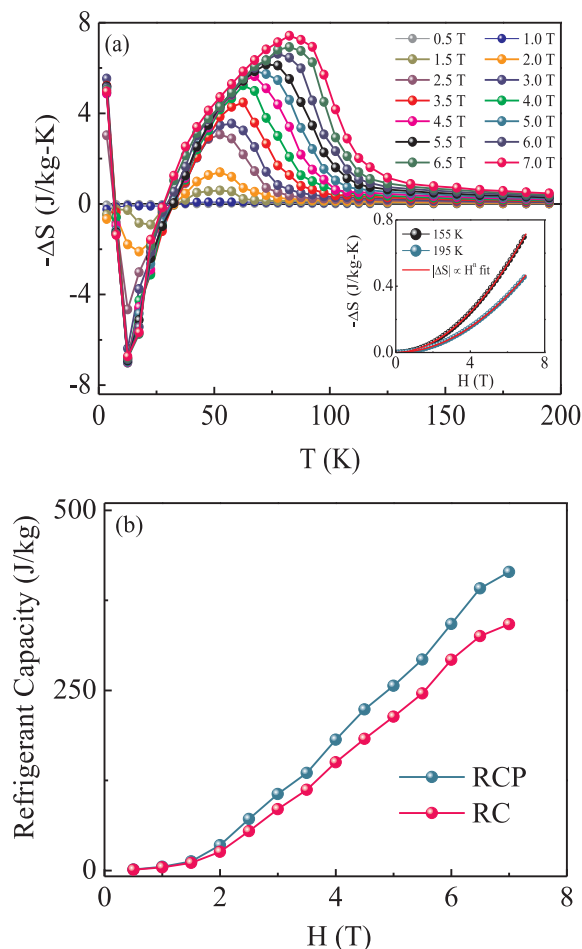


**Fig. 4.** (a) Temperature dependence of isothermal magnetic entropy change ( $\Delta S$ ) at different magnetic fields calculated by using Maxwell relation. Inset shows the  $H^2$  dependence of magnetic entropy change at paramagnetic temperature,  $T = 155$  K and 195 K, (b) Variation of refrigerant capacity (both RCP and RC) with magnetic fields.

$$\Delta S = \int_0^H \left( \frac{\partial M}{\partial T} \right) dH \quad (1)$$

We have calculated magnetic entropy change ( $\Delta S$ ) as a function of temperature at different values of external magnetic field. The variation of  $-\Delta S$  with temperature is shown in Fig. 4(a). This variation indicates the ferromagnetic nature of the compound for  $T > 30$  K. However,  $T < 30$  K, compound exhibits irregular nature. In this region,  $-\Delta S$  is negative even at the maximum magnetic field value. The origin of such anomalous nature of the magnetic entropy change at low temperature region is described at the latter part of this paper. It is known that  $\Delta S$  quadratically depends upon the magnetic field ( $\Delta S \propto H^2$ ) in the paramagnetic region [68]. To check this we have fitted the  $-\Delta S$  vs  $H$  curves at two different temperatures  $T = 155$  K and 195 K where the sample attains a paramagnetic state. From the inset of Fig. 4(a), it is clearly seen that our sample shows a  $H^2$  dependence on  $-\Delta S$  values at  $T = 155$  K and 195 K.

Apart from the change of magnetic entropy ( $\Delta S$ ), there are other important parameters have been used to describe the cooling capacity of a magnetic material namely, relative cooling power (RCP) and refrigerant capacity (RC) [69]. The net amount of heat transferred between a hot source and a cold sink in an ideal magnetic refrigeration cycle is defined as the cooling or refrigeration capacity of the material. Quantitatively the RCP and RC can be deduced by using following expressions

$$RCP = |\Delta S_{max}| \cdot (\Delta T)_{FWHM} \quad (2)$$

$$RC = \int_{T_1}^{T_2} |\Delta S| dT \quad (3)$$

where  $\Delta T_{FWHM}$  represents the full width at half maxima of temperature i.e  $\Delta T_{FWHM} = (T_2 - T_1)$ . The variation of RCP and RC with external magnetic field is shown in Fig. 4(b). Both RCP and RC value increases linearly with increasing applied magnetic fields. The RCP value is ominously large (415 J/kg) under a field change of 7 T.

One can observe from the temperature dependent of magnetization (M-T) curves (Fig. 2(a) and (b)) that our sample ESMO undergoes a paramagnetic to ferromagnetic phase transformation at certain temperatures depending upon the applied magnetic fields. At small magnetic fields, a thermal hysteresis appears in between ZFCW and FCW curves in the phase transforming region which directly indicates the existing of multiple magnetic phases and the magnetic transition associated with this can be correlated with first-order magnetic phase transition [70,71]. The thermal hysteresis is vanished with application of higher magnetic fields. Here we must mention that our system does not show any structural transition down to 15 K as proved by XRD spectrum as shown in Fig. 1(b). As reported by K. Xu et al. that the ferromagnetic phase fraction ( $f(T)$ ) can be calculated by considering the assumption that the total magnetization is proportional to the phase volume fraction [72]. Regarding this point, we must clear that we have only considered the magnetization data measured under FCW protocol to avoid the effect of thermal hysteresis present in the compound. In order to estimate the value of  $f(T)$ , it is essential to first get the magnetization data for fully ferromagnetic phase ( $M_{FM}$ ) as well as fully paramagnetic phase ( $M_{PM}$ ) at a given temperature. For this, we linearly extrapolated the as obtained M-T data in two different phases for different magnetic fields. These two obtained  $M_{FM}(T)$  and  $M_{PM}(T)$  curves can be seen in Fig. 5 as represented by green and orange dotted lines respectively. The ferromagnetic phase fraction  $f(T)$  can be calculated with the help of  $M(T)$ ,  $M_{FM}(T)$  and  $M_{PM}(T)$  by using the expression:

$$f(T) = \frac{M(T) - M_{PM}}{M_{FM} - M_{PM}} \times 100\% \quad (4)$$

The as obtained  $f(T)$  curve is plotted with respect to temperature for  $H = 5$  T as shown in Fig. 5, represented by red line. As reported by B. Emre et al., the effect of magnetic field and temperature is equivalent thermodynamically as a driving force for the change of magnetic phases [73]. In order to check this, we calculated  $f(T)$  for various magnetic fields from M-T data measured at  $H = 0.01$  T, 5 T and 7 T as shown in

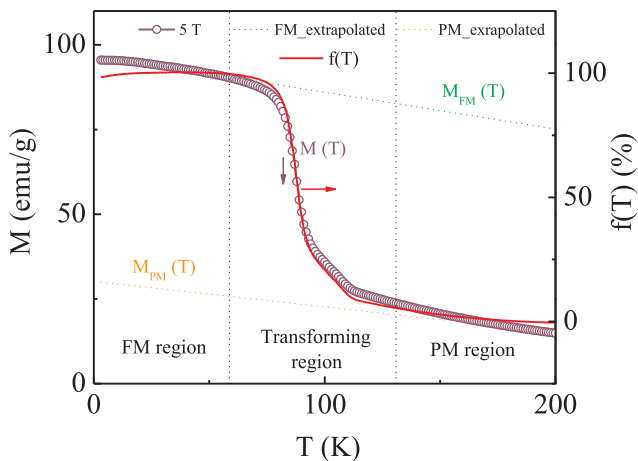


Fig. 5. Temperature dependence of magnetization curve represented by purple open circle of ESMO compound measured at  $H = 5$  T. The green and orange dotted lines represent the  $M_{FM}(T)$  and  $M_{PM}(T)$  respectively obtained from the linear extrapolation of the M-T data. The equivalent ferromagnetic phase fraction  $f(T)$  is represented by using solid red line.

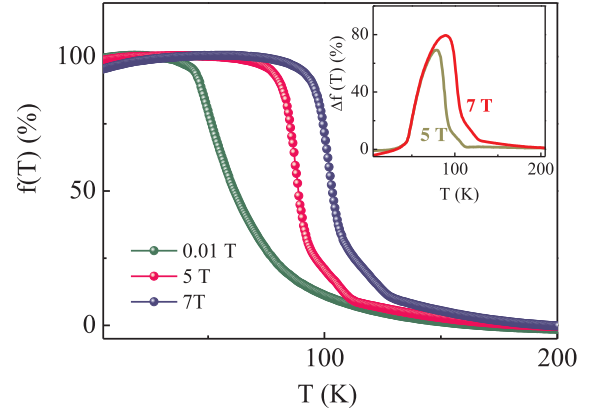


Fig. 6. Temperature dependence of ferromagnetic phase fraction  $f(T)$  at different magnetic fields. Inset shows the corresponding  $\Delta f(T)$  versus  $T$  curves calculated for the same magnetic fields.

Fig. 6. One can clearly see that the transition temperature ( $T_c$ ) is shifted towards higher temperature with increasing magnetic field as like  $M(T)$  curves although the shape of  $f(T)$  curves remain unchanged. Inset of Fig. 2(b) represent the magnetic field dependence of  $T_c$ .  $T_c$  linearly increases with increasing magnetic field. The slope of the curve ( $dT_c/dH$ ) is about 7.6 K/T. The change of ferromagnetic phase fraction or increment of ferromagnetism in the sample by increasing magnetic field can be quantified as  $\Delta f(T, \Delta H) = f(T, H_f) - f(T, H_i)$ , where  $H_i$  and  $H_f$  are the initial and final field values respectively [72]. In present case, we take 0.01 T as initial field and the calculated  $\Delta f(T, \Delta H)$  as a function of temperature is shown in the inset of Fig. 6.

The total entropy change ( $\Delta S$ ) in the vicinity of phase transition can be quantitatively estimated by using Clausius- Clapeyron equation [74-76] as given as

$$\Delta S = -\Delta M \left( \frac{dT_c}{dH} \right)^{-1} \quad (5)$$

where,  $\Delta M = M_{FM} - M_{PM}$  is the difference of magnetization in between complete FM phase and PM phase. Since the magnetic field directly affect the tendency of phase transformation, as a result the value of  $\Delta f(T, \Delta H)$  should involved in order to calculate the change of magnetic entropy as reported by K. Xu et al. [72]. Therefore, Eq. (5) can be rewritten as

$$\Delta S = -\Delta f \cdot \Delta M \left( \frac{dT_c}{dH} \right)^{-1} \quad (6)$$

We have calculated the change of magnetic entropy ( $\Delta S$ ) by using Eq. (6) for a field change of  $H = 5$  T and 7 T and compared the results with the as calculated entropy change by using Maxwell relation as shown in Fig. 7.

The temperature variation of magnetocaloric entropy change ( $-\Delta S$ ) under a field change of  $H = 5$  T and  $H = 7$  T indicates two different nature as obtained from two independent procedures. At low temperature region,  $-\Delta S$  is negative when it was calculated using Maxwell's Relation (MXR). However, the magnetic entropy change ( $-\Delta S$ ) deduced from Clausius-Clapeyron equation does not exhibit such nature (negative value at low temperatures).

Numerically, the negative value of  $-\Delta S$  was observed when magnetization get increased with increasing temperature. Generally for antiferromagnetic compounds, below the Neel temperature ( $T_N$ ), magnetization is increased with temperature and corroborates the negative value of  $-\Delta S$  at the low temperature region. However, for long ranged ferromagnetic compounds, at higher values of the external magnetic field, magnetization get reduced with the increasing of temperature which reveals a positive nature of the  $-\Delta S(T)$  vs  $T$  curve. A complicated scenario was appeared in case of the phase separated

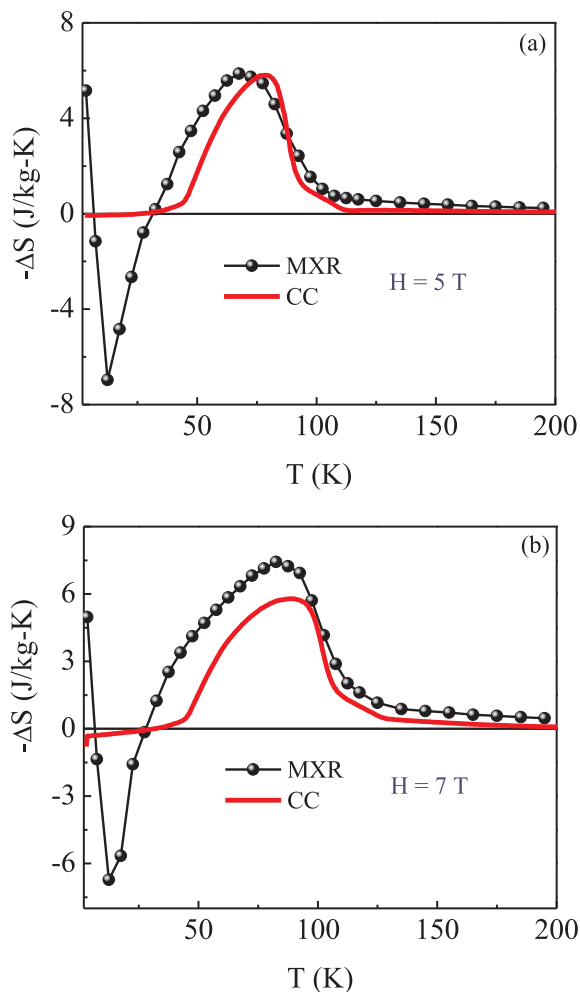


Fig. 7. Temperature dependence of isothermal magnetic entropy change calculated by using both Clausius-Clapeyron (CC) equation and Maxwell's relation (MXR) measured at (a)  $H = 5$  T and (b)  $H = 7$  T.

(ferromagnetic and antiferromagnetic) compounds having metamagnetic transition. For such compounds, below a particular magnetic field (critical magnetic field for metamagnetic transition), compounds exhibits antiferromagnetic properties. However, ferromagnetic nature was predominantly appears, above the critical magnetic field values [56,58,63]. For polycrystalline perovskite manganites, at very lower magnetic field the zero field cooled (ZFC) magnetization value increases with increasing temperature even in case of the ferromagnetic compounds up to spin blocking temperature ( $T_B$ ). Such nature of magnetization may be associated with grain boundary effect, pinning centers, defects, surface spin freezing etc. Generally to calculate the magnetic entropy change by MXR, the ZFC isotherms are used. Due to the anomalous nature of the magnetization at low temperature and low magnetic field, magnetic entropy change,  $-\Delta S$  achieved a negative value even for polycrystalline compounds. However in the presence of large external magnetic field, such nature generally diminished and predominant ferromagnetic correlation was obtained. In contrast to this, in our present study for ESMO compound, negative  $-\Delta S$  (calculated from MXR) was observed below 25 K even in the presence of the large magnetic field. For the sake of clarity we have plotted the variation of the  $-\Delta S(T)$  in the presence of 5 T and 7 T external magnetic field in Fig. 7. These result also compared with the same as calculated by using Clausius-Clapeyron equation which indicates the ferromagnetic nature of the compound. To concentrate about the origin of the anomalous results arises from MXR, it is important to mention that ZFC-FC bifurcation was present even up to 7 T external magnetic field. Such

nature in magnetization may be associated with the presence of the strong short range interaction of the compound. So from the above comparative study it may be argued that magnetocaloric effect deduced from Clausius-Clapeyron equation for such system having strong short range interaction is more realistic in nature.

#### 4. Conclusions

To summarize, we have carried out the magnetic and magnetocaloric properties of polycrystalline ESMO compound. Magnetocaloric effect of this compound have been calculated by using two different techniques. The observed discrepancy of magnetic entropy change (calculated from Maxwell's relation and Clausius-Clapeyron equation) were addressed considering the phase separated ground state of the compound. Additionally, the existence of the short range interaction markedly influenced the nature of the variation of magnetic entropy change as a function of temperature. Our study indicates a reliable pathway to calculate the magnetocaloric parameter like  $-\Delta S$  for any materials having irreversible nature in magnetization.

#### Declaration of Competing Interest

The authors declare that they have no known competing financial interests or personal relationships that could have appeared to influence the work reported in this paper.

#### Acknowledgements

The work was supported by Department of Atomic Energy (DAE), Govt. of India.

#### References

- [1] A.M. Tishin, Y.I. Spichkin, *The Magnetocaloric Effect and its Applications*, Institute of Physics Publishing, Bristol and Philadelphia, 2003.
- [2] K.A. Gschneidner Jr., V.K. Pecharsky, A.O. Tsokol, *Rep. Prog. Phys.* 68 (2005) 1479.
- [3] H. Wada, Y. Tanabe, M. Shiga, H. Sugawara, H. Sato, *J. Alloys Comp.* 316 (2001) 245.
- [4] J. Liu, T. Gottschall, K.P. Shokov, J.D. Moore, O. Gutfleisch, *Nat. Mater.* 11 (2012) 620.
- [5] H. Zeng, C. Kuang, J. Zhang, *Bull. Mater. Sci.* 34 (2011) 825.
- [6] H. Wada, Y. Tanabe, *Appl. Phys. Lett.* 79 (2001) 3302.
- [7] A.O. Pecharsky, K.A. Gschneidner Jr, V.K. Pecharsky, *J. Appl. Phys.* 93 (2003) 4722.
- [8] M.H. Phan, S.C. Yu, *J. Magn. Magn. Mater.* 308 (2007) 325.
- [9] A. Rostamnejadi, M. Venkatesan, P. Kameli, H. Salamati, J.M.D. Coey, *J. Magn. Magn. Mater.* 323 (2011) 2214.
- [10] B.G. Shen, J.R. Sun, F.X. Hu, H.W. Zhang, Z.H. Cheng, *Adv. Mater.* 21 (2009) 4545.
- [11] B.F. Yu, Q. Gao, B. Zhang, X.Z. Meng, Z. Chen, *Int. J. Refrig.* 26 (2003) 622.
- [12] V.K. Pecharsky, K.A. Gschneidner Jr., *Int. J. Refrig.* 29 (2006) 1239.
- [13] O. Tegus, E. Bruck, K.H.J. Buschow, F.R. De Boer, *Nature (London)* 415 (2002) 150.
- [14] E. Bruck, *J. Phys. D: Appl. Phys.* 38 (2005) R381.
- [15] D. Mazumdar, K. Das, S. Roy, I. Das, *J. Magn. Magn. Mater.* 497 (2020) 166066, <https://doi.org/10.1016/j.jmmm.2019.166066>.
- [16] T. Paramanik, T. Samanta, R. Ranganathan, I. Das, *RSC Adv.* 5 (2015) 47860.
- [17] R. M'nassri, *Phase Transitions* 90 (7) (2016) 687.
- [18] H. Zhu, C. Xiao, H. Cheng, F. Grote, X. Zhang, T. Yao, Z. Li, C. Wang, S. Wei, Y. Lei, Yi Xie, *Nat. Commun.* 5 (2014) 3960.
- [19] D.M. Polishchuk, Yu.O.T. Polishchuk, E. Holmgren, A.F. Kravets, A.I. Tovstolytnin, V. Korenivski, *Phys. Rev. Mater.* 2 (2018) 114402.
- [20] F. Cugini, G. Porcari, S. Fabbri, F. Albertini, M. Solzi, *Phil. Trans. R. Soc. A* 374 (2016) 20150306.
- [21] T. Paramanik, K. Das, T. Samanta, I. Das, *J. Appl. Phys.* 115 (2014) 083914.
- [22] T. Samanta, I. Das, S. Banerjee, *Appl. Phys. Lett.* 91 (2007) 152506.
- [23] S. Chatterjee, S. Giri, S. Majumdar, *J. Phys.: Condens. Matter* 24 (2012) 366001.
- [24] P. Sande, L.E. Hueso, D.R. Miguens, J. Rivas, *Appl. Phys. Lett.* 79 (2001) 2040.
- [25] A. Rostamnejadi, M. Venkatesan, J. Alaria, M. Boese, P. Kameli, H. Salamati, J.M.D. Coey, *J. Appl. Phys.* 110 (2011) 043905.
- [26] K. Rudolph, A.K. Pathak, Y. Mudryk, V.K. Pecharsky, *Acta Mater.* 145 (2018) 369.
- [27] D. Szweczyk, R. Thaljaoui, J. Mucha, P. Stachowiak, P. Vanderbenden, *Intermetallics* 102 (2018) 88.
- [28] J.S. Amaral, V.S. Amaral, *Appl. Phys. Lett.* 94 (2009) 042506.
- [29] M. Winklhofer, R.K. Dumas, K. Liu, *J. Appl. Phys.* 103 (2008) 07C518.
- [30] B.C. Zhao, Y.Q. Ma, W.H. Song, Y.P. Sun, *Phys. Lett. A* 354 (2006) 472.
- [31] V.K. Pecharsky, K.A. Gschneidner Jr., *Phys. Rev. Lett.* 78 (1997) 4494.

- [32] P. Zhang, T.L. Phan, S.C. Yu, *J. Supercond. Nov. Magn.* 25 (2012) 2727.
- [33] K. Das, I. Das, *J. Appl. Phys.* 119 (2016) 093903.
- [34] T. Tohei, H. Wada, T. Kanomata, *J. Magn. Magn. Mater.* 272 (2004) E585.
- [35] Y. Tokura, *Reports, Prog. Phys.* 69 (2006) 797.
- [36] M.B. Salamon, M. Jaime, *Rev. Mod. Phys.* 73 (2001) 583.
- [37] C.N.R. Rao, R. Raveau, *Colossal Magnetoresistance, Charge ordering and Related Properties of Manganese Oxides*, World Scientific, Singapore, 1998.
- [38] K. Das, P. Dasgupta, A. Poddar, I. Das, *Sci. Rep.* 6 (2016) 20351.
- [39] S. Jin, T.H. Tiefel, M. McCormack, R.A. Fastnacht, R. Ramesh, L.H. Chen, *Science* 264 (1994) 413.
- [40] S. Banik, K. Das, I. Das, *RSC Adv.* 7 (2017) 16575.
- [41] N.S. Bingham, M.H. Phan, H. Srikanth, M.A. Torija, C. Leighton, *J. Appl. Phys.* 106 (2009) 3.
- [42] V.Yu. Ivanov, A.A. Mukhin, A.S. Prokhorov, A.M. Balbashov, *Phys. Stat. Sol. (b)* 236 (2003) 445.
- [43] M. Respaud, J.M. Broto, H. Rakoto, J. Vanacken, P. Wagner, C. Martin, A. Maignan, B. Raveau, *Phys. Rev. B* 63 (2001) 144426.
- [44] K. Das, *J. Magn. Magn. Mater.* 458 (2018) 52.
- [45] A.I. Abramovich, L.I. Koroleva, A.V. Michurin, *J. Phys.: Condens. Matter* 14 (2002) L537.
- [46] T. Hashimoto, T. Numasawa, M. Shino, T. Okada, *Cryogenics* 21 (1981) 647.
- [47] V. Hardy, A. Maignan, S. Hebert, C. Martin, *Phys. Rev. B* 67 (2003) 024401.
- [48] R. Caballero-Flores, N.S. Bingham, M.H. Phan, M.A. Torija, C. Leighton, V. Franco, A. Conde, T.L. Phan, S.C. Yu, H. Srikanth, *J. Phys.: Condens. Matter* 26 (2014) 286001.
- [49] Y.R. Habarnau, P. Bergamasco, J. Sacanell, G. Leyva, C. Albornoz, M. Quintero, *Physica B* 407 (2012) 3305.
- [50] M. Aparnadevi, S.K. Barik, R. Mahendiran, *J. Magn. Magn. Mater.* 324 (2012) 3351.
- [51] M. Balli, O. Sari, D. Fruchart, J. Forchelet, *EPJ Web Conf.* 29 (2005) 00005.
- [52] L. Caron, Z.Q. Oub, T.T. Nguyen, D.T. Cam Thanh, O. Tegus, E. Bruck, *J. Magn. Magn. Mater.* 321 (2009) 3559.
- [53] A. Giguere, M. Foldeaki, B.R. Gopal, R. Chahine, T.K. Bose, A. Frydman, J.A. Barclay, *Phys. Rev. Lett.* 83 (1999) 2262.
- [54] G.J. Liu, J.R. Sun, J.Z. Wang, B.G. Shen, *Appl. Phys. Lett.* 89 (2006) 222503.
- [55] Y. Tadokoro, Y.J. Shana, T. Nakamura, S. Nakamura, *Solid State Ionics* 108 (1998) 261.
- [56] A. Sundaresan, A. Maignan, B. Raveau, *Phys. Rev. B* 55 (1997) 5596.
- [57] A.I. Abramovich, O.Yu. Gorbenko, A.R. Kaul, L.I. Koroleva, A.V. Michurin, *Phys. Solid State* 46 (2004) 1711.
- [58] J.Z. Wang, J.R. Sun, G.J. Liu, Y.W. Xie, D.J. Wang, T.Y. Zhao, B.G. Shen, X.G. Li, *Phys. Rev. B* 76 (2007) 104428.
- [59] G.J. Liu, J.R. Sun, Y.W. Xie, D.J. Wang, C.M. Xiong, H.W. Zhang, T.Y. Zhao, B.G. Shen, *Appl. Phys. Lett.* 87 (2005) 182502.
- [60] L. Jia, G.J. Liu, J.Z. Wang, J.R. Sun, H.W. Zhang, B.G. Shen, *Appl. Phys. Lett.* 89 (2006) 122515.
- [61] T.L. Phan, T.A. Ho, T.V. Manh, N.T. Dang, C.U. Jung, B.W. Lee, T.D. Thanh, *J. Appl. Phys.* 118 (2015) 143902.
- [62] D.N.H. Narn, R. Mathieu, P. Nordblad, N.V. Khiem, N.X. Phue, *Phys. Rev. B* 62 (2000) 1027.
- [63] D.S. Rana, R. Nirmala, S.K. Malik, *Europhys. Lett.* 70 (3) (2005) 376.
- [64] H. Aliaga, D. Magnoux, A. Moreo, D. Poiblan, S. Yunoki, E. Dagatto, *Phys. Rev. B* 68 (2003) 104405.
- [65] E. Dagotto, *Science* 309 (2005) 257.
- [66] S. Banik, K. Das, T. Paramanik, N.P. Lalla, B. Satpati, K. Pradhan, I. Das, *NPG Asia Mater.* 10 (2018) 923.
- [67] J. Dho, N.H. Hur, *Phys. Rev. B* 67 (2003) 214414.
- [68] H. Oesterreicher, F.T. Parker, *J. Appl. Phys.* 55 (1984) 4334.
- [69] V. Franco, J. Blazquez, B. Ingale, A. Conde, *Annu. Rev. Mater. Res.* 42 (2012) 305.
- [70] Z. Li, Y. Zhang, K. Xu, T. Yang, C. Jing, H.L. Zhang, *Solid State Commun.* 203 (2015) 81.
- [71] O. Gutfleisch, T. Gottschall, M. Fries, D. Benke, I. Radulov, K.P. Skokov, H. Wende, M. Gruner, M. Acet, P. Entel, M. Farle, *Philos. Trans. R. Soc. A* 374 (2016) 20150308.
- [72] K. Xu, Z. Li, Y.L. Zhang, C. Jing, *Phys. Lett. A* 379 (2015) 3149.
- [73] B. Emre, S. Yuce, E.S. Taulats, A. Planes, S. Fabbri, F. Albertini, L. Manosa, *J. Appl. Phys.* 113 (2013) 213905.
- [74] V. Recarte, J.I. Perez-Landazabalo, S. Kustov, E. Cesari, *J. Appl. Phys.* 107 (2010) 053501.
- [75] V.K. Pecharsky, K.A. Gshneidner Jr., A.O. Pecharsky, A.M. Tishin, *Phys. Rev. B* 64 (2012) 144406.
- [76] M. Balli, D. Fruchart, R. Zach, *J. Appl. Phys.* 115 (2014) 203909.